

A Cross-layer Communication Solution for Multimedia Applications in Underwater Acoustic Sensor Networks

Dario Pompili

Rutgers, The State University of New Jersey
Department of Electrical
and Computer Engineering
94 Brett Rd., Piscataway, NJ 08854
pompili@ece.rutgers.edu

Ian F. Akyildiz

Georgia Institute of Technology
School of Electrical and Computer Engineering
Broadband Wireless Networking Laboratory
75 5th St., Atlanta, GA 30308
ian@ece.gatech.edu

Abstract

Underwater multimedia acoustic sensor networks will enable new underwater applications such as multimedia coastal and tactical surveillance, undersea explorations, picture and video acquisition and classification, and disaster prevention. Because of the different requirements of these applications, it is needed to provide efficient differentiated-service support to delay-sensitive and delay-tolerant data traffic as well as to loss-sensitive and loss-tolerant traffic. The objective of this paper is twofold: 1) explore the interactions of different underwater communication functionalities such as modulation, forward error correction, medium access control and routing, and 2) develop a distributed cross-layer solution integrating specialized communication functionalities that cooperate to allow multiple devices to efficiently and fairly share the bandwidth-limited high-delay underwater acoustic medium.

1 Introduction

Underwater Acoustic Sensor Networks (UW-ASNs) [1] consist of sensors deployed to perform collaborative monitoring tasks over a body of water. UW-ASNs enable applications for oceanographic data collection, pollution monitoring, offshore exploration, and assisted navigation. Wireless acoustic communications are the typical physical layer technology in underwater networks due to radio frequency and optical waves propagation limitation. In addition to the ability to retrieve multimedia data, underwater multimedia sensor networks will also be able to store, process, correlate, and fuse data originated from heterogeneous sources. Thus, underwater multimedia sensor networks will not only enhance existing sensor network applications but they will also enable new applications such as multimedia coastal

and tactical surveillance, undersea explorations, picture and video acquisition and classification, and disaster prevention. Many of the above applications, however, require the underwater sensor network paradigm to be re-thought in view of the need for mechanisms to deliver multimedia content with a certain level of Quality of Service (QoS).

There are several characteristics of UW-ASNs that make QoS delivery of multimedia content a challenging task such as frequency-dependent transmission loss, colored noise, multipath, Doppler frequency spread, high and variable propagation delay, sensor battery and resource constraints, variable channel capacity, and cross-layer coupling of functionalities [1][9]. While most of research on underwater communication protocol design so far has followed the traditional layered approach, which was originally developed for wired networks, improved performance in wireless networks can be obtained with a cross-layer design, especially in a harsh environment such as the underwater.

Given our research experience in this area, in this paper we claim that UW-ASNs require for a cross-layer communication solution to allow for an efficient use of the scarce resources such as bandwidth and battery energy. However, although we advocate integrating *highly specialized* communication functionalities to improve network performance and to avoid *duplication of functions* by means of cross-layer design, it is important to consider the ease of design by following a *modular design approach*. This will also allow improving and upgrading particular functionalities without the need to re-design the entire communication system.

For these reasons, in this paper we rely on the above-mentioned design guidelines and propose a cross-layer communication solution for UW-ASN multimedia applications that is built upon our previous work on underwater routing [4] and Medium Access Control (MAC) [5]. In particular, the objective of this paper is twofold: 1) explore the interaction of different underwater communication

functionalities such as modulation, Forward Error Correction (FEC), MAC and routing, and 2) develop a distributed cross-layer solution integrating highly specialized communication functionalities that cooperate to allow multiple devices to efficiently and fairly share the bandwidth-limited high-delay underwater acoustic medium.

To the best of our knowledge, this work is the first to coherently propose a cross-layer framework to optimize communication within the UW-ASN paradigm. The remainder of the paper is organized as follows. In Sect. 2, we describe our design philosophy for cross-layering and we introduce our communication solution. In Sect. 3, we analyze the performance results. Finally, in Sect. 4, we draw the main conclusions and outline future research directions.

2 Cross-layer Communication Solution

Our objective is to develop a *resource allocation framework* that accurately models every aspect of the layered network architecture, resulting in theoretical and practical impacts beyond the previously established results. Our previous experience in modeling functionalities of the communication stack of underwater networks led us to develop a *highly specialized coherent communication solution* that can adapt to different application requirements and seek optimality in several different situations.

Our cross-layer solution relies on a distributed optimization problem to jointly control the *routing*, *MAC*, and *physical* functionalities in order to achieve efficient communications in the underwater environment. In particular, the proposed solution combines a 3D geographical routing algorithm (*routing functionality*), a novel hybrid distributed CDMA/ALOHA-based scheme to access the bandwidth-limited high-delay shared medium (*MAC functionality*), and an optimized solution for the *joint* selection of modulation, FEC, and transmit power (*physical functionalities*). The proposed solution is tailored for the characteristics of the underwater acoustic physical channel, e.g., it takes explicitly into account the very high propagation delay, which may vary in horizontal and vertical links due to multipath, the different components of the transmission loss, the impairment of the channel, the scarce and range-dependent bandwidth, the high bit error rate, and the limited battery capacity. These characteristics lead to very low utilization efficiencies of the underwater acoustic channel and high energy consumptions when common MAC and routing protocols are adopted in this environment, as analyzed in [4][5].

2.1 Physical Layer Functionalities

The underwater transmission loss describes how the acoustic intensity decreases as an acoustic pressure wave

propagates outwards from a sound source. The transmission loss $TL(d, f_0)$ [dB] that a narrow-band acoustic signal centered at frequency f_0 [kHz] experiences along a distance d [m] can be described by the Urlick propagation model [10],

$$TL(d, f_0) = \chi \cdot 10 \log_{10}(d) + \alpha(f_0) \cdot d. \quad (1)$$

In (1), the first term accounts for *geometric spreading*¹, which refers to the spreading of sound energy caused by the expansion of the wavefronts. It increases with the propagation distance and is independent of frequency. The second term accounts for *medium absorption*, where $\alpha(f_0)$ [dB/m] represents an absorption coefficient that describes the dependency of the transmission loss on the frequency.

Interestingly, the transmission loss increases not only with the transmission distance, but also with the signal frequency. As a result, given a maximum tolerated transmission loss TL_{max} [dB], which depends on the transmitter output power and the receiver sensitivity, a maximum central frequency exists for each range. In addition, because of the colored structure of the underwater ambient noise *power spectrum density* (*p.s.d.*), $N(f)$ [$\text{dB}_{re \mu Pa}/\text{Hz}$]², the useful acoustic bandwidth B [kHz]³ dramatically depends on the transmission distance and on the central frequency. Hence, the design of the routing and MAC functionalities of our cross-layer solution (Sect. 2.3) takes this characteristic of the underwater channel into account, which can be stated as follows: *a greater information throughput may be achieved if messages are relayed over multiple short hops instead of being transmitted directly over one long hop.*

Moreover, the unique ‘V’ structure of the underwater acoustic noise p.s.d. (which has a minimum of 20 $\text{dB}_{re \mu Pa}/\text{Hz}$ at about 40 kHz), makes *non-trivial* the choice of the optimal bandwidth. Interestingly, when the central frequency is low, e.g., $f_0 = 10$ kHz, a higher relative Signal-to-Noise-Ratio (*SNR*) is achieved with a narrow bandwidth ($B = 3$ as opposed to 9 kHz); conversely, when the central frequency is high, e.g., $f_0 = 100$ kHz, a higher relative *SNR* is achieved with a wide bandwidth ($B = 90$ as opposed to 30 kHz). This implies that if a high central frequency is used, a large bandwidth can be exploited for the communication, although a high transmit power would be needed to compensate for the higher transmission loss. Our communication solution takes into account this unique characteristic, which is caused by the peculiar ‘V’ structure of the noise p.s.d. and by the fact that the difference between the slopes of $N(f)$ and $TL(d, f)$ decreases as the

¹There are two kinds of geometric spreading: *spherical* (omni-directional point source, spreading coefficient $\chi = 2$), and *cylindrical* (horizontal radiation only, spreading coefficient $\chi = 1$).

²A reference pressure of $1 \mu Pa$ is used to express acoustic source levels in $\text{dB}_{re \mu Pa}$. Hence, 0.1, 1, and 10 W correspond to 161, 171, and 181 $\text{dB}_{re \mu Pa}$, respectively.

³We assume the band to be symmetrical around the central frequency, i.e., the band occupancy of bandwidth B at central frequency f_0 is $[f_0 - B/2, f_0 + B/2]$, which will be denoted as $\langle f_0, B \rangle$.

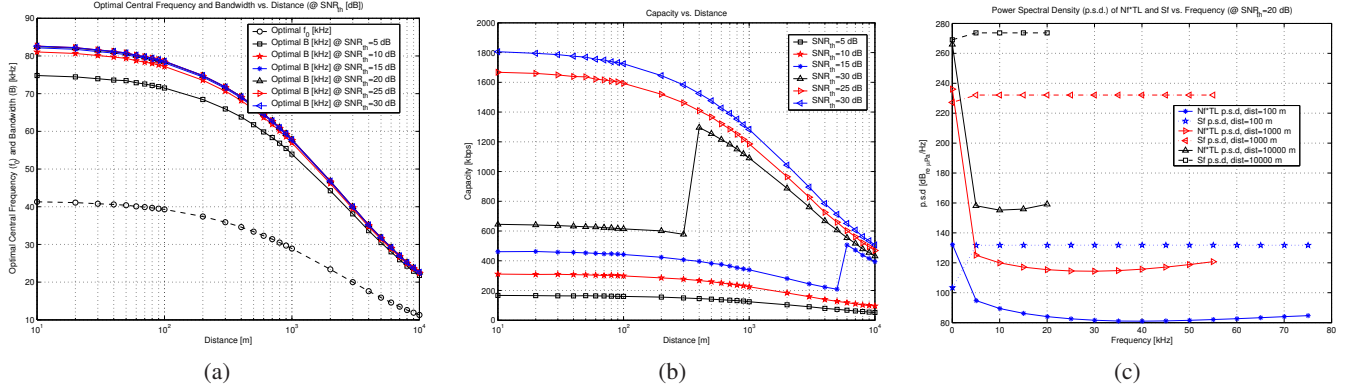


Figure 1. (a): Optimal central frequency f_0 [kHz] and chosen bandwidth B [kHz] vs. distance d [m], given a fixed pre-specified target $SNR_{th} \in [5, 30]$ dB; (b): Chosen capacity C [kbps] vs. distance d [m], given a fixed pre-specified target $SNR_{th} \in [5, 30]$ dB; (c): P.s.d. of $N(f) \cdot TL(d, f)$ and $S(d, f)$ [dB_{re μPa/Hz}] vs. frequency f [kHz] at $d = 10^2, 10^3, 10^4$ m when the pre-specified target SNR_{th} is heuristically set to 20 dB.

central frequency increases (e.g., positive for low frequencies and negative for high ones).

In [9], the author assesses the bandwidth dependency on the distance using an information-theoretic approach that takes into account the underwater propagation loss and ambient noise. The author defines the bandwidth corresponding to optimal signal energy allocation as the one that maximizes the channel link capacity. However, in order to find the optimal signal power distribution across the chosen band an a priori knowledge of the optimal SNR threshold (SNR_{th}) at the receiver is required, which is often a non-realistic assumption in practical systems. In [9], a heuristic pre-specified value of 20 dB is proposed for this threshold.

If we denote by $S(d, f)$ [dB_{re μPa/Hz}] the p.s.d. of the transmitted signal chosen for distance d , i.e., the power distribution across the chosen band $\langle f_0(d), B(d) \rangle$, then the total transmitted power is $P(d) = \int_{\langle f_0(d), B(d) \rangle} S(d, f) df$, and the signal to noise ratio is,

$$SNR(d, B(d)) = \frac{\int_{\langle f_0(d), B(d) \rangle} S(d, f) \cdot TL(d, f)^{-1} df}{\int_{\langle f_0(d), B(d) \rangle} N(f) df}. \quad (2)$$

By assuming that the noise is Gaussian and that the channel is time-invariant for some interval time, the channel transfer function appears frequency-nonselective in a narrow sub-band Δf centered around frequency f_i in which the noise can be approximated as white (with p.s.d. $N(f_i)$). Under these assumptions, the capacity C [bps] is given by,

$$C(d) = \sum_i \Delta f \log_2 \left[1 + \frac{S(d, f_i) \cdot TL(d, f_i)^{-1}}{N(f_i)} \right]. \quad (3)$$

Maximizing the capacity with respect to $S(d, f)$, subject to

the constraint that the transmitted power be finite, yields to the optimal p.s.d $S(d, f) = K(d) - N(f) \cdot TL(d, f)$, $f \in \langle f_0(d), B(d) \rangle$, according to the water-filling principle [6], where $K(d)$ [dB_{re μPa/Hz}] is a distance-dependent constant. The SNR corresponding to this optimal power distribution is thus given by,

$$SNR(d, B(d)) = K(d) \frac{\int_{f_0(d), B(d)} TL(d, f)^{-1} df}{\int_{f_0(d), B(d)} N(f) df} - 1. \quad (4)$$

Figure 1(a) depicts the chosen central frequency f_0 and bandwidth B , while Fig. 1(b) shows the associated theoretical capacity C , when a fixed pre-specified target SNR_{th} ranging in $[5, 30]$ dB is chosen. Note that, while the optimal central frequency f_0 (lower curve in Fig. 1(a)) is independent on the target SNR_{th} , both the chosen bandwidth B and maximum theoretical capacity C computed depend on it, which makes their values *suboptimal*. Therefore, the words ‘optimal’ and ‘chosen’. Figure 1(c) depicts the p.s.d. of $N(f) \cdot TL(d, f)$ and $S(d, f)$, as well as the signal band occupancy, when the pre-specified target SNR_{th} is heuristically set to 20 dB. This shows that, if the receiver SNR is not considered in the link optimization at the sender side, suboptimal decisions are taken. In fact, the link (and thus the overall system) performance strongly depends on the selected SNR_{th} , as it is emphasized in Figs. 1(a-c) and 2(a).⁴ For these reasons, our cross-layer solution *jointly controls*

⁴The discontinuity of the capacity as well as of the transmitted power in Figs. 1(b) and 2(a) at 300 and 5000 m, respectively, is caused by the minimum frequency $f_0 - B/2$ reaching zero, which in turns sets the maximum frequency to $f_0 + B/2$, given the constraint on the band symmetry around the central frequency.

physical transmission, modulation, and FEC functionalities, in such a way as to optimize the overall system performance by minimizing (or maximizing) meaningful objective functions such as the *energy per successfully received bit* (or the *net bit rate*), according to the application requirements.

In the next sections, we present the main communication functionalities of our cross-layer solution. Without the need for a target pre-specified SNR_{th} , our algorithm jointly selects, in a distributed manner, the optimal p.s.d. of the transmitted signal, i.e., K , f_0 , and B , and the best combination of modulation technique and FEC scheme as well as MAC and routing, with the objective of either saving energy, thus prolonging the lifetime of the network (*Objective 1*), or maximizing the system performance, thus increasing the network end-to-end throughput (*Objective 2*). Specifically, the actual objective (1 or 2) depends on the specific application requirements that need to be supported, and is either decided *offline* during the deployment phase, or *online* through control signaling from the surface station. In order to achieve the selected objective, our cross-layer communication solution interfaces with the modulation functionality by choosing the optimal transmitted power and number of bits per symbol, thus trading *power efficiency* for *spectral efficiency*⁵. Moreover, our solution interfaces with the FEC functionality, trading overhead, i.e., redundant bits, for increase of packet protection, i.e., bit error correcting capability (Sect. 2.2). Last but not least, it jointly decides the best next hop (routing functionality) and the modalities to access the channel and send the data to the chosen next hop (MAC functionality) (Sect. 2.3).

2.2 Modulation and FEC Interactions

We considered several classes of modulation schemes such as PSK, FSK, and QAM (both in their coherent and non-coherent versions), whose Bit Error Rate (BER) vs. SNR performance is reported in Fig. 2(b). Note that, while normally BER plots are referred to the received bit SNR E_b/N_0 , we define the p.s.d. of an equivalent white noise as $N_0 = (1/B) \cdot \int_{<f_0, B>} N(f)df$, and the received bit energy as $E_b = (1/C) \cdot \int_{<f_0, B>} S(d, f) \cdot TL(d, f)^{-1}df$. Hence, the equivalent bit SNR is $E_b/N_0 = (B/C) \cdot SNR$.

As far as the FEC functionality is concerned, we considered block codes because of their energy efficiency and lower complexity compared to convolutional codes [7][8]. In fact, the limited energy consumption requirements of UW-ASNs and the low complexity in the sensor hardware necessitate energy efficient error control and prevent high complexity codes to be implemented. In [8], the en-

⁵By moving to a higher-order constellation, it is possible to transmit more bits per symbol using the same bandwidth (*higher spectral efficiency*), although at the price of higher energy per bit required for a target Bit Error Rate (BER) (*lower power efficiency*).

ergy consumption profile of convolutional codes is presented based on μ AMPS architecture. It is shown that no convolutional code provides better energy efficiency for $BER > 10^{-5}$ than uncoded transmission [8]. Similarly, in [7], convolutional and BCH (Bose, Ray-Chaudhuri, Hocquenghem)⁶ codes are compared in terms of energy efficiency in a framework to optimize the packet size in wireless sensor networks. Results of this work reveal that BCH codes outperform the most energy efficient convolutional code by almost 15%. Consequently, we do not consider convolutional codes in our work, although our framework can be extended to support convolutional codes as well as other codes such as turbo codes or Type I or II Automatic Repeat reQuest (ARQ) schemes. Last but not least, the use of BCH codes leads to simple closed-form expressions to compute the Packet Error Rate (PER) given the link BER, which can be readily used for the purpose of the optimization carried out by the cross-layer solution proposed in this paper.

A BCH block code is represented by (n, k, t) , where n is the block length, k is the payload length, and t is the error correcting capability in bits. In our experiments, we used BCH codes able to correct up to $t = 10$ bit errors. Fig. 2(c) depicts PER vs. BER for different BCH(n,k,t) codes and for the case of uncoded transmissions (NO FEC), computed as,

$$\begin{cases} BLER(n, k, t) = \sum_{i=t+1}^n \binom{n}{i} BER^i \cdot (1 - BER)^{n-i}, \\ PER(L_P, n, k, t) = 1 - [1 - BLER(n, k, t)]^{\lceil \frac{L_P}{k} \rceil}, \end{cases} \quad (5)$$

where BLER represents the BLock Error Rate and L_P is the packet length, which is set to 100 Byte.

To qualitative understand how we capture the cross-layer interactions between the modulation and FEC functionalities to improve the link performance, let us consider the objective of these functionalities when they operate in isolation. The FEC functionality performs the so-called channel coding, i.e., introduces some controlled bit redundancy, with the objective of reducing the PER at the receiver given a certain BER on the link. On the other hand, the modulation functionality decides what the best modulation scheme and its constellation should be either i) to maximize the link raw rate, i.e., the rate of transmitted bits (spectrum efficiency), or ii) to minimize the link BER (power efficiency). It is clear that improved performance can be achieved by jointly selecting the BCH code and modulation scheme. Hence, our cross-layer design is aimed at maximizing the *link net rate*, i.e., the rate of *successfully* received bits, by jointly deciding: 1) the modulation scheme and its constellation (which affect the link raw rate), 2) the transmit power (which affects the BER), and 3) the FEC type and strength (which affect the PER). While this provides an intuitively

⁶A BCH code is a multilevel, cyclic, error-correcting, variable-length digital code used to correct multiple random error patterns.

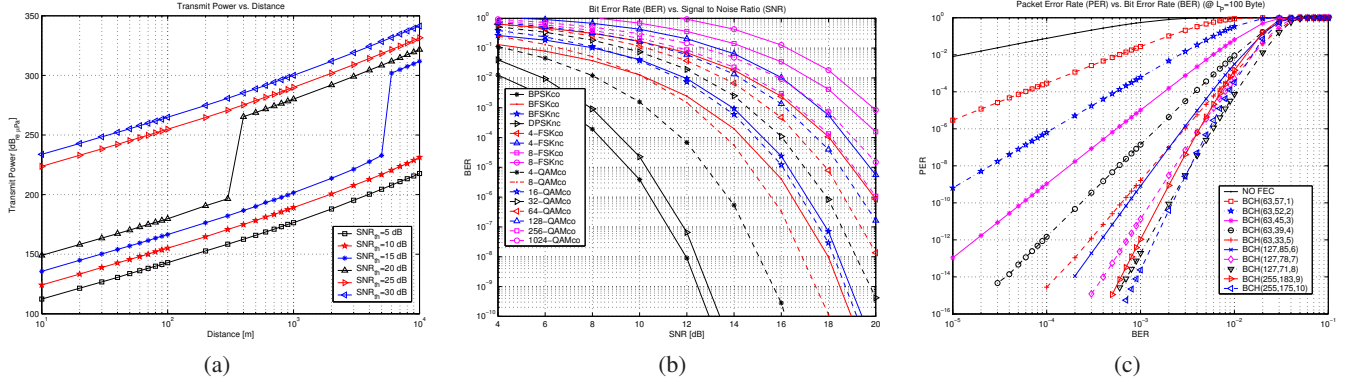


Figure 2. (a): Transmit power P [dB_{re μPa}] vs. distance d [m], given a fixed pre-specified target $SNR_{th} \in [5, 30]$ dB; (b): BER vs. SNR for different coherent and non-coherent typical underwater modulation techniques; (c): Packet error rate (PER) vs. BER for different BCH(n,k,t) codes.

explanation of the cross-layer operation as far as the physical layer functionalities are concerned, in the next sections we cast a rigorous mathematical framework to capture the FEC/modulation cross-layer interactions.

2.3 MAC and Routing Interactions

The MAC functionality is based on a novel *hybrid medium access scheme* that combines Direct Sequence Code Division Multiple Access (DS-CDMA) for the data payload and a simple yet effective ALOHA access for a control header, which is transmitted *back-to-back* immediately before the data packet to help the next hop set its receiver, as explained in Sect. 2.4. The MAC functionality incorporates a closed-loop distributed algorithm that interacts with the physical functionality, described in Sect. 2.1, to set the *optimal transmit power* and *code length*. The objective is to let signals arrive at the receiver with approximately the same mean power, thus minimizing the *near-far effect*⁷ [3].

DS-CDMA compensates for the effect of multipath, which may heavily affect underwater acoustic channels (especially in shallow water⁸), by exploiting the time diversity in the underwater channel. This leads to high channel reuse and low number of packet retransmissions, which result in decreased battery consumption and increased network throughput. In such a scheme, however, the major problem encountered is the Multiuser Access Interference (MAI), which is caused by simultaneous transmissions from different users. In fact, the system efficiency is limited by

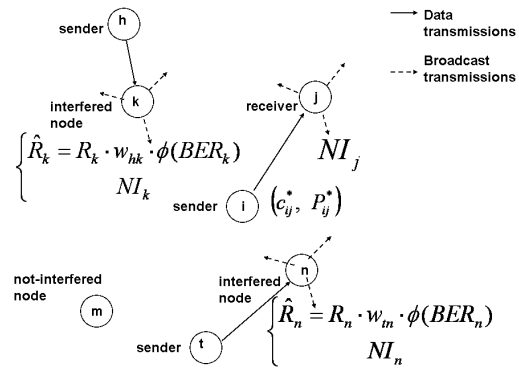


Figure 3. Data and broadcast transmissions.

the amount of total interference and not by the background noise exclusively [2]. Our MAC functionality, in conjunction with other functionalities such as FEC and modulation, aims at achieving three objectives, i.e., guarantee i) high network throughput, ii) low channel access delay, and iii) low energy consumption. To do so, it uses locally generated *chaotic codes* to spread transmitted signals on the optimal band, i.e., $\langle f_0^*, B^* \rangle$, which guarantees a flexible and granular bit rate, secure protection against eavesdropping, transmitter-receiver self-synchronization, and good auto- and cross-correlation properties.

The distributed closed-loop MAC functionality aims at setting the optimal combination of transmit power and code length at the transmitter side relying on local peri-

⁷The *near-far effect* occurs when the signal received by a receiver from a sender near the receiver is stronger than the signal received from another sender located further. In this case, the remote sender will be dominated by the close sender.

⁸In oceanic literature, shallow water refers to depth up to 100 m.

odic broadcasts of MAI values from active nodes, as shown in Fig. 3. Here, sender i needs to transmit on the shared medium a data packet to j , and let j receive enough power to correctly decode the signal without impairing ongoing communications from h to k and from t to n . Because the system efficiency is limited by the amount of total interference, it is crucial for i to optimize its transmission in terms of both transmit power and code length, in order to limit the near-far problem. These requirements are expressed by the following set of constraints,

$$\frac{\int NI_j(f) \cdot TL_{ij}(f) df}{w_{ij} \cdot \Omega(BER_{ij})} \leq P_{ij} \leq \min_{k \in \mathcal{K}_i} [(\hat{R}_k - NI_k) \cdot TL_{ik}]. \quad (6)$$

In (6), $NI_j(f)$ [W/Hz] is the noise plus MAI *p.s.d.* at receiver j , while NI_k [W] is the noise plus MAI *power* at nodes $k \in \mathcal{K}_i$, with \mathcal{K}_i being the set of nodes whose ongoing communications may be affected by node i 's transmit power. In addition, w_{ij} and $w_{t_k k}$ are the bandwidth spreading factors of the ongoing transmissions from i to j and from t_k to k , respectively, where t_k is the node from which k is receiving data. The normalized received spread signal, i.e., the signal power after despreading, is $\hat{R}_n = R_n \cdot w_{t_n n} \cdot \Omega(BER_{t_n n})$, where R_k [W] is the user signal power that receiver k is decoding, and $\Omega()$ is the MAI threshold, which depends on the target bit error rate. P_{ij} [W] represents the power transmitted by i to j . Finally, $TL_{ij}(f)$ and TL_{ik} are the transmission losses from i to j and from i to $k \in \mathcal{K}_i$, respectively, i.e., $TL_{ij}(f) = TL(d_{ij}, f)$ and $TL_{ik} = TL(d_{ik}, f_{0ik})$, as in (1).

The left constraint in (6) states that the SINR^{-1} at receiver j needs to be below a certain threshold, i.e., the power P_{ij} transmitted by i needs to be sufficiently high to allow receiver j to successfully decode it, given its current noise and MAI *p.s.d.* $NI_j(f)$. The right set of constraints in (6) states that the SINR^{-1} at receivers $k \in \mathcal{K}_i$ must be below a threshold, i.e., the power P_{ij} transmitted by i must not impair the ongoing communications toward nodes $k \in \mathcal{K}_i$. Consequently, to set its transmit power P_{ij} and spreading factor w_{ij} ⁹, node i needs to leverage information on the MAI and normalized receiving spread signal of neighboring nodes. This information is broadcast periodically by active nodes. In particular, to limit such broadcasts, a generic node n transmits only significant values of NI_n and \hat{R}_n , i.e., out of predefined tolerance ranges. Constraints (6) are incorporated in the cross-layer link optimization problem $\mathbf{P}_{\text{layer}}^{\text{cross}}(\mathbf{i}, \mathbf{j})$ in (16).

In our cross-layer solution, the level of interference at potential receivers, i.e., their MAI, is used not only by the MAC functionality, but also by the routing functionality to

⁹We assume the spreading factor to be proportional to the chaotic code length, i.e., $w_{ij} = \alpha \cdot c_{ij}$. By using *chaotic codes* as opposed to *pseudorandom sequences*, a much higher granularity in the code length can be achieved; code lengths, in fact, do not need to be a power of 2.

decide for the best next hop. In fact, while a routing functionality implemented in isolation would find the best path from the sender to the destination only considering routing-layer metrics, our cross-layer routing/MAC solution finds the best path also considering the interference levels at the neighboring nodes (potential next hops). This means that *a longer path characterized by a higher number of hops (or, in general, a path that would be suboptimal according to only routing-layer information) may be chosen if the direct path, i.e., the one that would guarantee the minimum number of hops, were composed of nodes characterized by high levels of MAI*, which would require longer codes and/or higher transmit power. Also, given the fact that in underwater acoustic channels the link bandwidth increases when the range decreases (i.e., shorter links provide higher bandwidth, which in turns leads to higher data rates, as discussed in Sect. 2.1), our cross-layer design solution captures this interactions between the routing and physical-layer functionalities by trying to compose, in a distributed manner, paths using short links to exploit their higher bandwidth. This cross-layer approach leads to a higher end-to-end throughput, as shown in Sect. 3.

The proposed routing functionality relies on a geographical paradigm, which is very promising underwater for its scalability feature and limited required signaling. However, Global Positioning System (GPS) radio receivers, which may be used in terrestrial systems to accurately estimate the geographical location of sensor nodes, do not work properly in the underwater environment. Still, underwater devices need to estimate their current position, as it is necessary to associate the sampled data with the 3D position of the device that generates the data to spatially reconstruct the characteristics of the event. Underwater localization can be achieved by leveraging the low speed of sound in water, which permits accurate timing of signals, and pairwise node distance data can be used to perform 3D localization.

According to our distributed routing algorithm, a source or relay node i will select j^* as its best next hop iff

$$j^* = \begin{cases} \underset{OR}{\operatorname{argmin}}_{j \in \mathcal{S}_i \cap \mathcal{P}_i^N} E_i^{(j)*} & \text{(Objective 1)} \\ \underset{OR}{\operatorname{argmax}}_{j \in \mathcal{S}_i \cap \mathcal{P}_i^N} R_i^{(j)*} & \text{(Objective 2)}, \end{cases} \quad (7)$$

where $E_i^{(j)*}$ [J/bit] represents the minimum energy required to successfully transmit a payload bit from node i to the sink and $R_i^{(j)*}$ [bps] represents the maximum net bit rate that can be achieved from node i considering every outbound links in the path towards the sink. In (7), \mathcal{S}_i is the *neighbor set* of node i and \mathcal{P}_i^N is the *positive advance set*, which is composed of nodes closer to sink N than node i , i.e., $j \in \mathcal{P}_i^N$ iff $d_{jN} < d_{iN}$. The link metrics $E_i^{(j)*}$ and $R_i^{(j)*}$ in (7) are the objective functions (8) and (9) of the cross-layer link optimization problem

$P_{\text{layer}}^{\text{cross}}(\mathbf{i}, \mathbf{j})$. These metrics take into account the number of packet transmissions \hat{N}_{ij}^T associated with the optimal link (i, j^*) , given the optimal combination of modulation technique $(M_{ij}^* \in \mathcal{M})$ and FEC $(F_{ij}^* \in \mathcal{F}, L_{P_{ij}}^F)$, and transmitted p.s.d. $S_{ij}^*(f) = K_{ij}^* - NI_{j^*}(f) \cdot TL_{ij^*}(f)$, $f \in \langle f_{0ij^*}^*, B_{ij^*}^* \rangle$. Moreover, they account for the estimated hop-path length \hat{N}_{ij}^{Hop} from node i to the sink when j^* is selected as next hop.

The proposed optimization problem is a distributed communication solution for different multimedia traffic classes that optimizes the transmission considering every feasible outbound link from i , i.e., (i, j) , $j \in \mathcal{S}_i \cap \mathcal{P}_i^N$, by choosing the optimal p.s.d. of the transmitted signal as well as band (K^*, f_0^*, B^*) , modulation (M^*) , FEC (F^*, L_P^F) , and code length (c^*) . The objective is set depending on the high-level application requirements. We consider two alternate objectives, i.e., *Objective 1*: minimize the energy per bit transmitted; and *Objective 2*: maximize the link net bit rate, defined as the link bit rate R^b discounted by the number of transmissions N^T . While the first objective leads to prolong the lifetime of the network, the second leads to high end-to-end throughput. In the following, we cast the cross-layer link optimization problem.

$P_{\text{layer}}^{\text{cross}}(\mathbf{i}, \mathbf{j})$: Cross-layer Link Optimization Problem

Find : $K_{ij}^*, f_{0ij}^*, B_{ij}^*, M_{ij}^*, F_{ij}^*, L_{P_{ij}}^F, c_{ij}^*$

Objective 1 : Minimize $\mathbf{E}_i^{(j)} = \mathbf{E}_{ij}^b \cdot \Pi_{ij}^{e2e}$ (8)

OR Objective 2 : Maximize $\mathbf{R}_i^{(j)} = \mathbf{R}_{ij}^b \cdot \Pi_{ij}^{e2e}^{-1}$ (9)

Subject to :

(Class-independent Constraints/Relationships)

$$R_{ij}^b = \frac{\eta(M_{ij}) \cdot B_{ij}}{c_{ij}}, \quad E_{ij}^b = 2E_{elec}^b + \frac{P_{ij}}{R_{ij}^b} \quad (10)$$

$$\Pi_{ij}^{e2e} = \frac{L_P^*}{L_P^* - L_P^H - L_{P_{ij}}^F} \cdot \hat{N}_{ij}^T \cdot \hat{N}_{ij}^{Hop} \quad (11)$$

$$SINR_{ij} = K_{ij} \frac{\int_{f_{0ij}, B_{ij}} TL_{ij}(f)^{-1} df}{\int_{f_{0ij}, B_{ij}} NI_j(f) df} - 1 \quad (12)$$

$$BER_{ij} = \Phi^{M_{ij}}(SINR_{ij}) \quad (13)$$

$$PER_{ij} = \Psi^{F_{ij}}(L_P^*, L_{P_{ij}}^F, BER_{ij}) \quad (14)$$

$$\hat{N}_{ij}^{Hop} = \max\left(\frac{d_{iN}}{\langle d_{ij} \rangle_{iN}}, 1\right) \quad (15)$$

$$P_{ij}^{min}(c_{ij}, BER_{ij}) \leq P_{ij} \leq \min[P_{ij}^{max}, P_i^{max}] \quad (16)$$

where

$$P_{ij} = K_{ij} \cdot B_{ij} - \int_{\langle f_{0ij}, B_{ij} \rangle} NI_j(f) \cdot TL_{ij}(f) df \quad (17)$$

$$P_{ij}^{min}(c_{ij}, BER_{ij}) = \frac{\int_{\langle f_{0ij}, B_{ij} \rangle} NI_j(f) \cdot TL_{ij}(f) df}{\alpha \cdot c_{ij} \cdot \Omega(BER_{ij})} \quad (18)$$

$$P_{ij}^{max} = \min_{k \in \mathcal{K}_i} [(\hat{R}_k - NI_k) \cdot TL_{ik}] \quad (19)$$

(Class-dependent Constraints/Relationships)

$$\text{Class I} = \begin{cases} \hat{N}_{ij}^T = 1 \\ 1 - (1 - PER_{ij})^{[\hat{N}_{ij}^{Hop} + N_{HC}^{(m)}]} \leq PER_{max}^{e2e, (m)} \end{cases}$$

$$\text{Class II} = \left\{ \hat{N}_{ij}^T = (1 - PER_{ij})^{-1} \right.$$

$$\text{Class III} = \begin{cases} \hat{N}_{ij}^T = 1 \\ 1 - (1 - PER_{ij})^{[\hat{N}_{ij}^{Hop} + N_{HC}^{(m)}]} \leq PER_{max}^{e2e, (m)} \\ \frac{\tilde{d}_{ij}}{q_{ij}} + \delta(\gamma) \cdot \sigma_{ij}^q \leq \left(\frac{\Delta D_{ij}^{(m)}}{\hat{N}_{ij}^{Hop}}\right) - \hat{Q}_{ij} - \frac{L_P^*}{R_{ij}^b} \end{cases}$$

$$\text{Class IV} = \begin{cases} \hat{N}_{ij}^T = (1 - PER_{ij})^{-1} \\ \frac{\tilde{d}_{ij}}{q_{ij}} + \delta(\gamma) \cdot \sigma_{ij}^q \leq \left(\frac{\Delta D_{ij}^{(m)}}{\hat{N}_{ij}^{Hop}}\right) - \hat{Q}_{ij} - \frac{L_P^*}{R_{ij}^b} \end{cases}$$

We envision that underwater multimedia sensor networks will need to provide support and differentiated service to applications with different QoS requirements, ranging from delay-sensitive to delay-tolerant, and from loss-sensitive to loss-tolerant. Hence, we consider the following four traffic classes: **Class I** (delay-tolerant, loss-tolerant), **Class II** (delay-tolerant, loss-sensitive), **Class III** (delay-sensitive, loss-tolerant), and **Class IV** (delay-sensitive, loss-sensitive). While for loss-sensitive applications a packet is locally retransmitted until it is correctly decoded at the receiver, for loss-tolerant applications packets are transmitted only once on each link, and are protected unequally, depending on the importance of the data they are carrying for correct perceptual reconstruction.

Notations used in the *class-independent constraints/relationships*:

- $L_P^* = L_P^H + L_{P_{ij}}^F + L_{P_{ij}}^N$ [bit] is the *fixed* optimal packet size, solution of an *offline* optimization problem presented in [4], where L_P^H is the header size of a packet, while $L_{P_{ij}}^F$ is the *variable* FEC redundancy of each packet from i to j .
- $E_{elec}^b = E_{elec}^{trans} = E_{elec}^{rec}$ [J/bit] is the *distance-independent* energy to transit one bit, where E_{elec}^{trans} is the energy per bit needed by transmitter electronics (PLLs, VCOs, bias currents) and digital processing, and E_{elec}^{rec} represents the energy per bit utilized by receiver electronics.
- E_{ij}^b [J/bit] is the energy to transmit one bit from i to j , when the transmitted power and the bit rate are P_{ij} [W] and R_{ij}^b [bps], respectively. The second term P_{ij}/R_{ij}^b is the *distance-dependent* portion of the energy to transmit a bit.
- P_i^{max} [W] is the maximum transmitting power for node i .

- $BER = \Phi^M(SINR)$ represents the bit error rate, given the SINR and the modulation scheme $M \in \mathcal{M}$, while $\eta(M)$ is the modulation spectrum efficiency.
- $PER = \psi^F(L_P, L_P^F, BER)$ represents the link packet error rate, given the packet size L_P , the FEC redundancy L_P^F , and the bit error rate (BER), and it depends on the adopted FEC technique $F \in \mathcal{F}$.
- \hat{N}_{ij}^T is the number of transmissions of a packet sent by i .
- $\hat{N}_{ij}^{Hop} = \max(\frac{d_{iN}}{\langle d_{ij} \rangle_{iN}}, 1)$ is the estimated number of hops from node i to the surface station (sink) N when j is selected as next hop, and $\langle d_{ij} \rangle_{iN}$ is the projection of d_{ij} onto the line connecting node i with the sink.

Notations used in the *class-dependent constraints/relationships*:

- $PER_{max}^{e2e,(m)}$ is the maximum allowed end-to-end packet error rate to packet m , while N_{max}^{Hop} is the maximum expected number of hops.
- $N_{HC}^{(m)}$ is the hop count, which reports the number of hops of packet m from the source to the current node.
- $\Delta D_i^{(m)} = D_{max} - (t_{i,now}^{(m)} - t_0^{(m)}) [s]$ is the time-to-live of packet m arriving at node i , where $t_{i,now}^{(m)}$ is the arriving time of m at i , and $t_0^{(m)}$ is the time m was generated, which is time-stamped in the packet header by its source, and $D_{max} [s]$ is the maximum end-to-end delay.
- $T_{ij} = L_P^*/R_{ij}^b + T_{ij}^q [s]$ accounts for the packet transmission delay and the propagation delay associated with link (i, j) ; we consider a Gaussian distribution for T_{ij} , i.e., $T_{ij} \sim \mathcal{N}(L_P^*/R_{ij}^b + T_{ij}^q, \sigma_{ij}^q{}^2)$;
- $\hat{Q}_{ij} [s]$ is the network queuing delay estimated by node i when j is selected as next hop, computed according to the information carried by incoming packets and broadcast by neighboring nodes.

Note that sender i optimally decouples the routing decision, which is based on (7), from the solution of $\mathbf{P}_{layer}^{cross}(\mathbf{i}, \mathbf{j})$, whose output is the optimal metric $E_i^{(j)*}$ (or $R_i^{(j)*}$), input of the routing decision itself. Therefore, sender i can optimally decouple the cross-layer algorithm into two *sub-problems*: first, minimize the link metric $E_i^{(j)}$ (or maximize $R_i^{(j)}$) for each of its feasible next-hop neighbors (Algorithm 1 presents a possible space-search approach) (*physical functionalities*); second, pick as best next hop that node j^* associated with the best link metric (*MAC/Routing functionalities*). This means that the generic node i does not have to solve a complicated optimization problem to find its best route towards a sink. Rather, it only needs to sequentially solve the two aforementioned sub-problems *with no loss of optimality*. The first has a complexity $O(|\mathcal{S}_{th}| \cdot |\mathcal{M}| \cdot |\mathcal{F}|)$, where $|\mathcal{S}_{th}|$, $|\mathcal{M}|$, and $|\mathcal{F}|$

are the number of different SNR_{th} thresholds, modulation techniques, and FEC schemes, respectively, used in combination with Algorithm 2. The second has a complexity $O(|\mathcal{S}_i \cap \mathcal{P}_i^N|)$, i.e., proportional to the number of the sender's neighboring nodes with positive advance towards the sink. Moreover, this operation does not need to be performed every time a sensor has to route a packet, but only when the channel or the traffic conditions, i.e., the structure of the MAI in the neighborhood, have consistently changed.

Algorithm 1 Cross-layer Link Optimization (given i, j, d_{ij})

```

1:  $E_{min} = \infty$  [or  $R_{max} = 0$ ] {initialization}
2: for th=1 :  $|\mathcal{S}_{th}|$  do
3:   for mo=1 :  $|\mathcal{M}|$  do
4:     for fe=1 :  $|\mathcal{F}|$  do
5:        $(SNR, K, f_0, B) \leftarrow$  Algo 2( $SNR_{th} = th$ )
6:        $PER = \psi^{fe}(L_P, L_P^F(fe), \Phi^{mo}(SINR))$ 
7:       Solve  $\mathbf{P}_{layer}^{cross}$ , Calculate  $E_i^{(j)}$  (8) [OR  $R_i^{(j)}$  (9)]
8:       if ( $E_i^{(j)} < E_{min}$ ) [OR  $R_i^{(j)} > R_{max}$ ] then
9:          $E_{min} = E_i^{(j)}$  [OR  $R_{max} = R_i^{(j)}$ ]
10:         $(fe, mo, K, f_0, B)^* = (fe, mo, K, f_0, B)$ 
11:       end if
12:     end for {end FEC cycle}
13:   end for {end modulation cycle}
14: end for {end SNR cycle}
```

Algorithm 2 Link Transmission (given d and SNR_{th})

```

1:  $f_0 = \text{argmin}_f [N(f) \cdot TL(d, f)]$  {optimal  $f_0$ }
2:  $K^{(0)} = [\min_f N(f)] \cdot TL(d, f_0)$  {initialization}
3:  $stop = 0, n = 0$ 
4: while ( $stop == 0$ ) do
5:    $n = ++$ , Find  $B^{(n)}$  s.t.  $K^{(n-1)} \geq N(f) \cdot TL(d, f)$ 
6:   Calculate  $SNR^{(n)}$  from (4) using  $K^{(n-1)}$  and  $B^{(n)}$ 
7:   if ( $SNR^{(n)} \geq SNR_{th}$ ) then
8:      $stop = 1$ 
9:   else
10:     $K^{(n+1)} = (1 + \epsilon) \cdot K^{(n)}$   $\{\epsilon \in \mathbb{R}^+\}$ 
11:   end if
12: end while
```

2.4 Protocol Operation

Once the cross-layer optimization problem has been solved at sender i , and the *optimal communication parameters* (i.e., K^* , f_0^* , B^* , M^* , F^* , L_P^{F*} , and c^*) have been found, i randomly access the channel transmitting a short header called *Extended Header (EH)*. The EH is sent using a *common chaotic code* c_{EH} known by all devices. Sender i transmits to its next hop j^* the short header EH. The EH contains information about the final destination, i.e., the surface station, the chosen next hop, i.e., j^* , and the parameters that i will use to generate the *chaotic spreading code* of

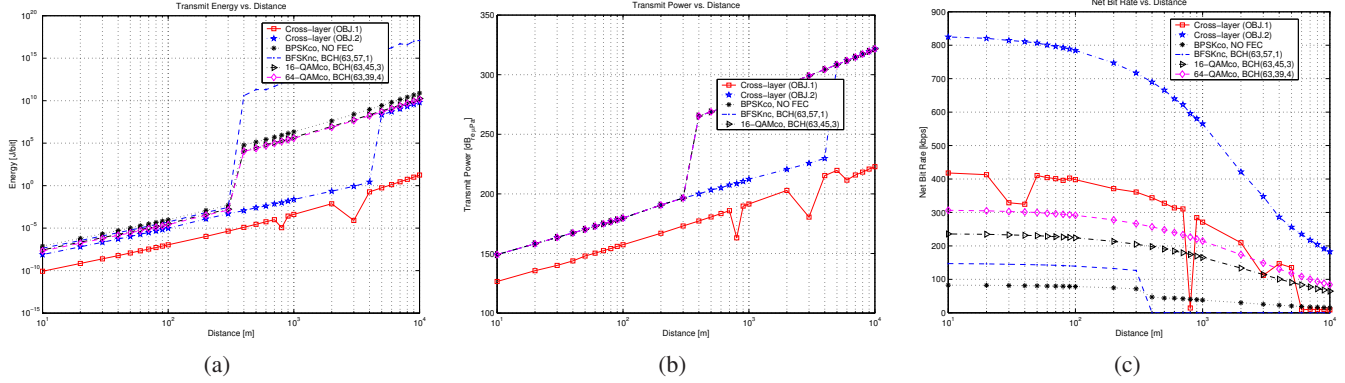


Figure 4. (a): Energy per bit $E_i^{(j)}$ [J/bit] (a), transmit power P [dB_{re μPa}] (b), and net bit rate $R_i^{(j)}$ [kbps] (c) vs. distance d [m] for the proposed cross-layer solution (Objectives 1 and 2) and for four fixed FEC/modulation combinations.

length c^* for the actual data packet that j^* will receive from i . Immediately after the transmission of the EH, i transmits the data packet on the channel using the *optimal communication parameters* set by the cross-layer algorithm.

Note that the protocol does not have to send control packets before the actual data packet is transmitted. This is because the packet - composed of the extra header EH and the actual data packet (payload plus standard header) - uses a hybrid MAC to access the channel, i.e., it simultaneously accesses the channel using ALOHA-like MAC (the header) and locally adapting its power and code length as in standard distributed CDMA MACs (data packet). This novel approach is motivated by the huge propagation delay affecting the underwater environment (five orders of magnitude larger than in terrestrial wireless networks) and by the need to achieve high channel utilization efficiencies to compensate for the low-bandwidth shared medium.

If no collision occurs during the reception of the EH, i.e., if i is the only node transmitting an EH in the neighborhood of node j^* , j^* will be able to synchronize to the signal from i , despread the EH using the common code, and acquire the carried information. Then, if the EH is successfully decoded, receiver j^* will be able to locally generate the chaotic code that i used to send its data packet, and set its decoder according to the optimal communication parameters used by i in such a way as to decode the data packet. Once j^* has correctly received the packet from i , it acknowledges it by sending an ACK packet to j using code c_A . In case i does not receive the ACK before a timeout T_{out} expires, it will keep transmitting the packet until a maximum transmission number is reached. If sender i does not have updated information about the MAI in j^* , it increases the code length every time a timeout expires to improve the probability that the packet be decoded.

3 Performance Evaluation

In this section we compare the performance achieved by our-cross layer solution against that achieved by individual communication functionalities that do not share information and operate in isolation. Also, we compare results obtained when the objective function of our cross-layer optimization problem is either Objective 1 or 2.

As far as the interactions between physical layer functionalities are concerned, Fig. 4 shows the energy per bit $E_i^{(j)}$ [J/bit] (a), transmit power P [dB_{re μPa}] (b), and net bit rate $R_i^{(j)}$ [kbps] (c) vs. distance d [m] for the proposed cross-layer solution (when both Objective 1 and 2 - in the figures OBJ.1 and OBJ.2 - are considered) and for those four fixed FEC/ modulation combinations that showed best performance. As can be seen, our solution outperforms competing fixed schemes when either objective is selected, in terms of both energy and throughput. In particular, in Figs. 4(a) and 4(b), the curves associated with OBJ.1, representing the transmit energy and power, respectively, for a payload bit to be successfully decoded at the receiver, are always above any other curve associate with a fixed FEC/ modulation combination such as coherent BPSK/NO FEC, non-coherent BFSK/BCH(63,57,1), coherent 16-QAM/BCH(63,45,3), and coherent 16-QAM/BCH(63,39,4). Moreover, the performance gain of our cross-layer solution over the best FEC/ modulation combination out of the four considered increases as the distance increases. Note that, out of the many FEC/ modulation combinations we tested, for the sake of clarity, in the figures we reported only those four with best performance. The same conclusion can be drawn looking at Fig. 4(c), which reports the net bit rate vs. distance for

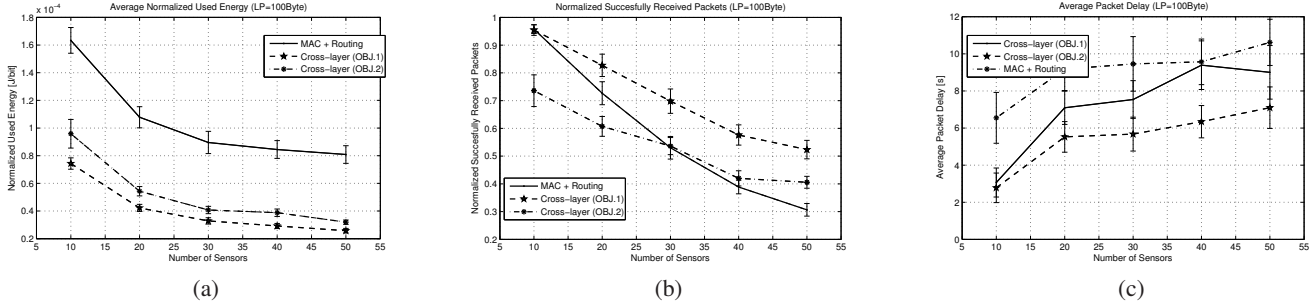


Figure 5. (a): Average normalized energy vs. no. of sensors (Class II); (b): Normalized successfully received packets vs. no of sensors (Class II); (c): Average packet delay vs. no. of sensors (Class III).

our solution as well as for the best four competing fixed schemes. Again, the curve depicting the performance of our solution when OBJ.2 is set as objective function of the optimization problem outperforms any of the other four curves whatever distance is considered.

As far as the interactions between MAC and Routing functionalities are concerned, Figs. 5(a-c) report the average normalized used energy, the normalized successfully received packets, and the average packet delay, respectively, vs. number of sensors. We considered a variable number of sensors (from 10 to 50) randomly deployed in a 3D volume of $500 \times 500 \times 500 \text{ m}^3$. Performance results refer to the three cases of OBJ.1 and OBJ.2 for our cross-layer solution, and the case where a CDMA-based MAC [5] and geographically-based routing [4] run individually. In Figs. 5(a-b) our cross-layer solution with OBJ.1 outperforms the MAC+Routing case (Class II), and in Fig. 5(c) this is again the case with OBJ.2 (Class III). These positive results are due to the fact that our solution jointly optimizes the considered communication functionalities, thus leveraging synergies that lead to improved end-to-end system performance.

4 Conclusions and Future Work

We explored the interaction of different underwater communication functionalities, and developed a cross-layer communication solution that allows for efficient utilization of the bandwidth-limited high-delay underwater acoustic channel. We showed that end-to-end network performance improves in terms of both energy and throughput when highly specialized communication functionalities are integrated in a cross-layer module. As future work, we shall develop an ad-hoc scheduling mechanism to simultaneously handle traffic classes with different QoS requirements, and we shall incorporate end-to-end rate control functionalities to provide fair congestion avoidance in dynamic conditions.

References

- [1] I. F. Akyildiz, D. Pompili, and T. Melodia. Underwater Acoustic Sensor Networks: Research Challenges. *Ad Hoc Networks (Elsevier)*, 3(3):257–279, May 2005.
- [2] C.-S. Chang and K.-C. Chen. Medium Access Protocol Design for Delay-guaranteed Multicode CDMA Multimedia Networks. *IEEE Transactions on Wireless Communications*, 2(6):1159–1167, Nov. 2003.
- [3] A. Muqattash, M. Krunz, and W. E. Ryan. Solving the Near-far Problem in CDMA-based Ad Hoc Networks. *Ad Hoc Networks (Elsevier)*, 1(4):435–453, Nov. 2003.
- [4] D. Pompili, T. Melodia, and I. F. Akyildiz. Routing Algorithms for Delay-insensitive and Delay-sensitive Applications in Underwater Sensor Networks. In *Proc. of ACM Conference on Mobile Computing and Networking (MobiCom)*, Los Angeles, LA, Sept. 2006.
- [5] D. Pompili, T. Melodia, and I. F. Akyildiz. A Distributed CDMA Medium Access Control for Underwater Acoustic Sensor Networks. In *Proc. of Mediterranean Ad Hoc Networking Workshop (Med-Hoc-Net)*, Corfu, Greece, June 2007.
- [6] J. Proakis. *Digital Communications*. McGraw-Hill, New York, 2000.
- [7] Y. Sankarasubramaniam, I. F. Akyildiz, and S. W. McLaughlin. Energy Efficiency Based Packet Size Optimization in Wireless Sensor Networks. In *Proc. of IEEE Internal Workshop on Sensor Network Protocols and Applications (SNPA)*, Seattle, WA, May 2003.
- [8] E. Shih, S.-H. Cho, N. Ickes, R. Min, A. Sinha, A. Wang, and A. Chandrakasan. Physical Layer Driven Protocol and Algorithm Design for Energy-efficient Wireless Sensor Networks. In *Proc. of ACM International Conference on Mobile Computing and Networking (MobiCom)*, Rome, Italy, July 2001.
- [9] M. Stojanovic. On The Relationship Between Capacity and Distance in an Underwater Acoustic Communication Channel. In *Proc. of ACM International Workshop on Underwater Networks (WUWNet)*, Los Angeles, CA, Sept. 2006.
- [10] R. J. Urick. *Principles of Underwater Sound*. McGraw-Hill, 1983.